High Energy Resummation at Hadronic Colliders

Jack J. Medley

A thesis submitted in fulfilment of the requirements
for the degree of Doctor of Philosophy
to the
University of Edinburgh
March 2016

Abstract

Abstract abstract.

Declaration

Except where otherwise stated, the research undertaken in this thesis was the unaided work of the author. Where the work was done in collaboration with others, a significant contribution was made by the author.

J. Medley
March 2016

Acknowledgements

Cheers guys!

Contents

List of Figures

List of Tables

Chapter 1

Introduction

1.1 A Little History

The current 'Standard Model' of particle physics was completed in June 2012 with the announcement of the Higgs boson by the ATLAS collaboration. This discovery with the final piece needed to complete the picture developed over the course of the past century beginning with the discovery of the electron in 1897.

The Standard Model is a gauge quantum field theory describing three of the four observed fundamental forces - with the inclusion of gravity remaining elusive. The local gauge structure is given by[1]:

$$SU(3)_c \times SU(2)_L \times U(1)_Y. \tag{1.1}$$

The $SU(3)_c$ group describes the strong nuclear force (Quantum Chromodynamics or QCD) and the 8 gauge generators give us the massless spin-1 gluons, $G^{\mu}_{a}(x)$ $a = 1, \ldots, 8$, present in the standard model. There are three states, $W^{\mu}_{a}(s)$ $a = 1, \ldots, 3$, associated with the $SU(2)_L$ group and a further one, $B^{\mu}(x)$, coming from the $U(1)_Y$ group.

The only remaining boson to complete the standard model arises from the complex scalar Higgs field who's ground state is not invariant under the action of $SU(2)_L \times U(1)_Y$. This field breaks the standard model gauge symmetry to

[1]The subscripts on the groups are simply a convenient notation. The 'c' on $SU(3)$ acts to remind us that it is the strong 'colour' coupling being described. The 'L' on $SU(2)$ indicates that all right-handed states are in the trivial representation of the group and the 'Y' on the $U(1)$ is a reminder that this is the hypercharge group and not the electromagnetic group.

$$SU(3)_c \times U(1)_{em}, \tag{1.2}$$

where now the $U(1)$ refers to the electromagnetic charge. After the 'Spontaneous Symmetry Breaking' occurs the four aforementioned bosons, $W_a^\mu(s)$ and $B^\mu(x)$ acquire mass and combinations of them are physically realised as the experimentally observer electroweak boson; The massive states $W^\pm, Z^0$ and the massless photon, γ. The photon and the Z^0 bosons are of particular importance in the work that follows.

The fundamental particle content of the Standard Model also includes fermions. These are spin-1/2 particles which obey the spin-statistics theorem (and hence the Pauli exclusion principle) and comprise all known visible matter in the universe. The fermions are structured in three so-called 'generations', shown in table 1.1 and can be further subdivided in to quarks and leptons. Quarks are colour triplets under QCD but are also charged under the electroweak group. The up (u), charm (c) and top (t) quarks have electric charge $+\frac{2}{3}$ while the down (d), strange (s) and bottom (b) quarks have $-\frac{1}{3}$. Leptons are singlets under $SU(3)$ and so do not couple to the strong sector. The charged leptons e, μ and τ have electric charge -1 and the neutrinos are neutral.

	First Generation	Second Generation	Third Generation
Quarks	u, d	c, s	t,
Leptons	e, ν_e	μ, ν_μ	τ, ν_τ

Table 1.1: The fermion content of the standard model.

1.2 Thesis Outline

The aim of this thesis is to detail the importance of a certain class of perurbatively high-order terms in events with QCD radiation in the final state. In particular we will consider corrections to parton-parton collisions with a Z^0 or γ in association with high energy QCD radiation in the final state.

In chapter 2 I will begin by introduce quantum chromodynamics, the theory of the strong sector in the standard model, and detail how we might use this to calculate physical observables (such as cross-sections and differential

distributions) at hadron colliders such as the Large Hadron Collider. I will discuss how these observables fall prey to divergences in QCD-like quantum field theories with massless states and mention briefly how such divergences can be handled. I will then describe how the computationally expensive integrals derived in subsequent chapters may be efficiently evaluated using Monte-Carlo techniques.

In chapter 3 the details of QCD in the 'High Energy' limit are discussed. After completing a few instructive calculations we will see how, in this limit, the traditional fixed-order perturbation theory view of calculating cross-sections fades as another subset of terms, namely the 'Leading Logarithmic' contributions, become more important. I will discuss previous work in the High Energy limit of QCD and how this can be used to factorise complex parton-parton scattering amplitudes into combinations of 'currents' which, when combined with gauge-invariant effective gluon emission terms can be used to construct approximate high-multiplicity matrix elements.

In chapter 4 the work of the previous chapter is extended to the case where there is a massive Z^0 boson or an off-shell photon, γ^*, in the final state. A 'current' for this process is derived and the complexities arising from two separate sources of interference are explored. This new result is for the matrix element is compared to the results obtained from a Leading Order (in the strong coupling, α_s) generator `MadGraph` at the level of the matrix element squared in wide regions of phase space is seen to be in good agreement. This result must then be regularised to treat the divergences discussed in chapter 2 and this process is presented. The procedure for matching this regularised result to well-known Leading Order results is shown and the importance of the inclusion of these non-resummation terms is discussed. Lastly three comparisons of the High Energy Jets Z+Jets Monte-Carlo generator to recent experimental studies `ATLAS` and `CMS` at the LHC are shown.

In chapter 5 we apply the massive spinor-helicity to the production of a $t\bar{t}$ pair in hadronic collisions. Using the `PySpinor` package we calculate values for the full-mass matrix element and compare them to leading-order (in α_s) results from `MadGraph`. This is a process in which the leading logarithmic contribution starts at one order higher than in previous work and so the effects of the resummation are not as expected to be as crucial as in the case of chapter 4 - however at large values for the centre-of-mass energy (such as that a future high energy circular collider) these 'next-to-leading' logarithms will once again lead to the breakdown

of fixed-order perturbation theory.

In chapter 6 we discuss the results of a lengthy study of jet production from the ATLAS collaboration. This analysis was a thorough look at BFKL-like dynamics in proton-proton colliders and the HEJ predictions are seen to describe the data well in the regions of phase-space where we know the effects of our resummation become relevant.

From here we move towards comparisons with experiments using the results of chapter 4, and the resulting publicly available Monte Carlo package, to a recent experimental prediction of the ratio of the $W^{\pm}$+jets rate to the Z/γ^*+jets rate. Our predictions are compared against next-to-leading order (in α_s) results from NJet and leading order results from MadGraph.

In chapter 8, with a study of Z/γ^*+Jets at a centre-of-mass energy of 100TeV relevant for the discussion of the next wave of high energy particle physics experiments (such as any Future Circular Collider) which are of great interest to the community at large. We see....DO THE STUDY BEFORE WRITING THIS!

Finally, in chapter 9 I summarise the results of the above chapters and provide a short outlook for future work.

Chapter 2

QCD at hadronic colliders

2.1 The QCD Lagrangian

The Lagrangian for QCD is more complicated than the one previously seen for QED. This is in part due to us having to sum over different representations of the generating group, $SU(3)$, but mainly because the fields no longer commute with one another (they are non-Abelian in nature) and this leads to gauge boson self-interactions. The full Lagrangian is as follows [**?**] [1]:

$$\mathcal{L}^{QCD} = \overline{\psi}^i \left(i \not{D}^{ij} - m\delta^{ij} \right) \psi^j - \frac{1}{4} F^a_{\mu\nu} F^{a\mu\nu} - \frac{1}{2\xi} (\partial^\mu A^a_\mu)^2 + (\partial^\mu \chi^{a*}) \mathcal{D}^{ab}_\mu \chi^b. \quad (2.1a)$$

$$D^{ij}_\mu = \delta^{ij} \partial_\mu - i g_s (T^c)^{ij} A^c_\mu. \quad (2.1b)$$

$$\mathcal{D}^{ab}_\mu = \delta^{ab} \partial_\mu - g_s f^{abc} A^c_\mu. \quad (2.1c)$$

where the indices i, j run from 1 to 3, the indices a, b, c run from 1 to 8, D_μ is the covariant derivative in the fundamental representation, $\mathcal{D}_\mu$ is the covariant derivative in the adjoint representation, T^a are the generating matrices and finally $f^{abc} = i(T^a_{adj})^{bc}$. The χ fields are the 'ghost' excitations and their origin will be explained in section 3.1.

In analogy to section (2) we begin by decomposing equation (12) into a free Lagrangian and an interacting Lagrangian as follows:

[1] With the bare quantity subscripts supressed

$$\mathcal{L}_0^{QCD} = \overline{\psi}^i \left(i\partial\!\!\!/ - m\right)\psi^i - \frac{1}{4}\partial_{[\mu}A^a_{\nu]}\partial^{[\mu}A^{\nu]a} - \frac{1}{2\xi}(\partial^\mu A^a_\mu)(\partial^\nu A^a_\nu) + (\partial^\mu \chi^{a*})(\partial_\mu \chi^a), \tag{2.2}$$

$$\mathcal{L}_I^{QCD} = g_s\overline{\psi}^i T^a_{ij}\gamma^\mu\psi^j - \frac{g_s}{2}f^{abc}\partial_{[\mu}A^a_{\nu]}A^{b\mu}A^{c\nu} - \frac{g_s^2}{4}f^{abe}f^{cde}A^a_\mu A^b_\nu A^{c\mu}A^{d\nu} - g_s f^{abc}\partial^\mu\chi^{a*}\chi^b A^c_\mu. \tag{2.3}$$

By calculating the QCD partition function and acting with the appropriate derivatives we can find the fermion propagator and the ghost propagator, repectively:

$$\langle 0|\psi_i(x)\psi_j(y)|0\rangle = S_F(x-y) = \int \frac{d^4k}{(2\pi)^4}e^{-ik\cdot(x-y)}\delta_{ij}\frac{i}{k\!\!\!/ - m + i\epsilon}, \tag{2.4}$$

$$\langle 0|\chi_a(x)\chi_b(y)|0\rangle = H_F(x-y) = \int \frac{d^4k}{(2\pi)^4}e^{-ik\cdot(x-y)}\delta_{ab}\frac{i}{k^2 + i\epsilon}. \tag{2.5}$$

and we can read off the various QCD vertex factors directly from the interaction Lagrangian.

2.1.1 The Faddeev-Popov Procedure for NAGTs

All that remains to be done is to evaluate the gluon propagator. As in QED when trying to compute the propagator of a massless gauge boson we can use the work of Faddeev and Popov. The functional integral we want to evaluate is in the form:

$$\int DA e^{-\frac{i}{4}\int d^4x F^a_{\mu\nu}F^{a\mu\nu}}. \tag{2.6}$$

Where $DA = \prod_x \prod_{a,\mu} dA^a_\mu$. As briefly outlined above we would like to perform a functional integration over all possible gauge choices and then pick out the subset of gauges we are interested in by enforcing the gauge condition $G(A) = 0$ to eliminate overcounting. This constraint may be written as [**?**]:

$$\int D\alpha(x)\delta(G(A^\alpha))Det\left(\frac{\delta G(A^\alpha)}{\delta\alpha(x)}\right) = 1. \tag{2.7}$$

Where $A^\alpha_\mu = A_\mu - \frac{1}{g_s}\partial_\mu\alpha(x)$. Making a gauge transformation ($A_\mu \to A^\alpha_\mu$) and inserting equation (18):

$$\int DAe^{-\frac{i}{4}\int d^4F^a_{\mu\nu}F^{a\mu\nu}} = \int DA\int D\alpha(x)\delta(G(A^\alpha))Det\left(\frac{\delta G(A^\alpha)}{\delta\alpha(x)}\right)e^{-\frac{i}{4}\int d^4F^a_{\mu\nu}F^{a\mu\nu}}, \tag{2.8a}$$

$$= \int D\alpha(x)\int DA\delta(G(A^\alpha))Det\left(\frac{\delta G(A^\alpha)}{\delta\alpha(x)}\right)e^{-\frac{i}{4}\int d^4F^a_{\mu\nu}F^{a\mu\nu}}. \tag{2.8b}$$

We are free to change the functional integration variable to A^α_μ since everything is gauge invariant leading to an integrand which *only* depends on A^α_μ. We can therefore simply relabel back to A_μ:

$$= \left(\int D\alpha(x)\right)\int DA\delta(G(A))Det\left(\frac{\delta G(A)}{\delta\alpha(x)}\right)e^{-\frac{i}{4}\int d^4F^a_{\mu\nu}F^{a\mu\nu}}. \tag{2.9}$$

The functional integration can now just be factored out as a constant and we can choose the function $G(A)$ as a generalisation of the Lorentz gauge: $G(A) = \partial^\mu A^a_\mu - \omega^a$. This choice leads us to the correct gluon propagator - along with our free parameter, ξ:

$$\langle 0|A_a(x)A_b(y)|0\rangle = G^{\mu\nu}_F(x-y) = \int\frac{d^4x}{(2\pi)^4}e^{-ik\cdot(x-y)}\delta_{ab}\frac{-i}{k^2+i\epsilon}\left(g^{\mu\nu} - (1-\xi)\frac{k^\mu k^\nu}{k^2}\right). \tag{2.10}$$

but because the QCD gauge transformation is more involved than the QED eqivalent the determinant term still depends on A_μ:

$$Det\left(\frac{\delta G(A)}{\delta\alpha(x)}\right) = Det\left(\frac{\partial_\mu D^\mu}{g_s}\right). \tag{2.11}$$

We can however simply invent another type of field and choose to write out determinant as

$$Det\left(\frac{\delta G(A)}{\delta\alpha(x)}\right) = \int D\chi D\overline{\chi}e^{i\int d^4x\overline{\chi}(-\partial_\mu D_\mu)\chi}. \tag{2.12}$$

These non-physical modes are called the Faddeev-Popov ghosts/antighosts and are a consequence of enforcing gauge invariance - they are represented by the final term in equation (12a).

2.1.2 Renormalising the QCD Lagrangian

Similarly to QED we anticipate divergent quantities in our calculations above tree level and so we introduce counterterms into our Lagrangian. Similarly to equation (4) we have the following relations:

$$\psi_0 = Z_\psi^{\frac{1}{2}}\psi, \qquad A_0^a = Z_A^{\frac{1}{2}}A^a, \qquad \chi_0^a = Z_\chi^{\frac{1}{2}}\chi^a, \tag{2.13a}$$

$$m_0 = Z_m m, \qquad g_{s0} = Z_s g_s, \qquad \xi_0 = Z_\xi \xi. \tag{2.13b}$$

Inserting these into equations (13) and (14) and rearranging so that we have $\mathcal{L}^{\mathcal{QCD}} = \mathcal{L}_0 + \mathcal{L}_{ct}$ where $\mathcal{L}_0$ is as definied in equation (13) and the counterterm Lagrangian is:

$$\begin{aligned}\mathcal{L}_{ct} = &-(Z_A - 1)\frac{1}{4}(F_{\mu\nu}^a)^2 + (Z_\chi - 1)i(\partial^\mu\chi^a)(\partial_\mu\chi^a) + (Z_\psi - 1)\overline{\psi^i}(i\partial\!\!\!/ - m)\psi^i - Z_\psi(Z_m - 1)m\overline{\psi^i}\psi \\ &-(Z_s Z_A^{\frac{3}{2}} - 1)\frac{1}{2}g_s f^{abc}\partial_{[\mu}A_{\nu]}^a A^{b\mu}A^{c\nu} - (Z_s^2 Z_A^2 - 1)\frac{1}{4}g_s^2 f^{abe}f^{cde}A_\mu^a A_\nu^b A^{c\mu}A^{d\nu} - \dots \\ &-(Z_s Z_\chi Z_A^{\frac{1}{2}} - 1)ig_s f^{abc}(\partial^\mu\chi^a)\chi^b A_\mu^c + (Z_s Z_\psi Z_A^{\frac{1}{2}} - 1)g_s\overline{\psi}^i T_{ij}^a\gamma^\mu\psi^j A_\mu^a.\end{aligned} \tag{2.14}$$

2.2 Factorisation at Hadronic Colliders

2.3 A brief look at divergences and regularisation

In calculations above tree level we encounter divergences of various kinds which can be divided up into three classes:

- Ultraviolet (UV) divergences: These occur when all the components of a loop momenta tend to infinity, $k^\alpha \to \infty$, such that k^2 becomes the dominant term in propagator. Since these extrememly high momentum modes corresponding to physics at very short distance scales we choose to interpret these divergences as an indication that our theory is only an effective theory and we shouldn't attempt to apply it to all scales.

- Infrared (IR) divergences: These occur in theories with massles gauge

bosons, such as QED and QCD, since a particle may emit any number of arbitrarily such bosons with infinitesimal energy and we would never be able to detect their emission. In contrast to the UV divergences the IR becomes important in the region of phase space where $k^2 \to 0$.

- Collinear (mass) divergences: These occur when we have massless bosons *and* have massless on-shell particles in our calculation. This can happen when we have, for example, a photon/gluon in the final state or the energy scale of the interaction is far higher than the mass of an emitted particle which admits taking that particles mass to be zero. We can see this by considering a typical propagator factor:

$$\frac{1}{(p+k)^2 - m^2} \sim \frac{1}{(p+k)^2} = \frac{1}{2p \cdot k} = \frac{1}{2E_p E_k(1 - \cos\theta_{pk})}. \tag{2.15}$$

  Where we have used the on-shell relations $p^2 = 0$ and $k^2 = 0$. Clearly as the angle of emission, θ_{pk}, tends to zero (the collinear limit) this term will diverge.

If we are to extract any useful information above tree-level we will have to find ways to control these infinities. We call these methods 'regularisation schemes'

2.3.1 Regularisation Schemes

The general plan with all regularisation schemes is to introduce a new parameter to the calculation which is used to get a handle on exactly *how* the integral diverges. Once we have performed the integration we take the limiting case where the effect of the regulator vanishes we will see that the divergence now presents itself as some singular function of the regulator when $\Lambda^2 \to \infty$. There are many ways to regularise divergences each with their own advantages and disadvantages. We will describe a few here:

- Hard momentum cut-off: In the hard momentum cut-off approach we simply replace the upper bound with some finite large value, Λ^2. This will regulate the UV and allow us to complete the calculation provided there are no IR or mass singularities. While this method is very conceptually simple it does break both translational invariance and gauge invariance which is far from ideal.

- Pauli-Villars regularisation: In the Pauli-Villars scheme we replace the normal propagators with propagators damped by a large mass:

$$\frac{1}{p^2 - m^2} \to \frac{1}{p^2 - m^2} - \frac{1}{p^2 - M^2}. \tag{2.16}$$

  For $m \ll M$. Once again this does not deal with any problems with the IR/mass singularities and in order to get this extra contributions we must add another field to our lagrangian which satifies the opposite statistics to the field we are trying to regulate.

- Mass regularisation: When using mass regularisation we give the gauge bosons a small mass to control any IR or mass divergences which might be present, we can then perform the integrals and the singularity re-emerges when we take the limit of massless bosons again. The disadvantage of this scheme is that it does not regulate the UV region of phase space and massive gauge bosons are forbidden by gauge invariance unless we have a broken symmetry.

- Dimensional regularisation: In dimensional regularisation we analytically continue the number of space-time dimensions away from the standard $d = 4$. We still want to be able to return to our usual 4D theory so we choose $d = 4 - 2\epsilon$ where ϵ is the regulator and we plan to take the limit $\epsilon \to 0$. The advantage of this is that dimensional regularisation treats both the UV and the IR divergences and both translational invariance and gauge invariance are preserved. However, this modification changes the well known Dirac algebra relations which makes computing the numerator slightly more involved. There are also some tensors which cannot easily be generalised to arbitrary dimensions.

2.3.2 The QCD Beta function

What is the beta function? Why is it important? How is the Beta function defined? What are the 5 diagrams needed to calculate the QCD beta function? Calculate a couple of these as an example - importance of result? Show that QCD CAN be treated perturbatively! Yaaay

2.4 Perturbative QCD and Resummation

2.4.1 Expansions in the strong coupling constant

2.4.2 An Example Fixed-Order Calculation

2.4.3 Limitations of Fixed-Order Schemes

2.4.4 Resumming Higher-Order Corrections

What would a dijet NLO calculation look like in a traditional α_s perturabtive expansion? A few diagrams maybe? A succesful prediction followed by a couple of examples where fixed order is misguided: $n_{njets} \to 3$, $d\phi$ of hardest two jets

2.5 Spinor-Helicity Notation

It is convenient to work in Helicity-Spinor notation to evaluate Feynman diagrams in the MRK limit [**?**]. As usual we have:

$$| \, p\pm\rangle = \psi_{\pm}(p) \qquad\qquad \overline{\psi_{\pm}(p)} = \langle p\pm \, | \, . \tag{2.17}$$

Often the helicity information will be supressed, and we define the following shorthand:

$$\langle pk\rangle = \langle p- \mid k+\rangle \qquad\qquad [pk] = \langle p+ \mid k-\rangle. \tag{2.18}$$

In this scheme we have the following identities:

$$\langle ij\rangle[ij] = s_{ij} \qquad \langle i\pm \mid \gamma^\mu \mid i\pm\rangle = 2k_i^\mu \tag{2.19}$$

$$\langle ij\rangle = -\langle ji\rangle \qquad [ij] = -[ji] \tag{2.20}$$

$$\langle ii\rangle = 0 \qquad [ii] = 0 \tag{2.21}$$

$$\langle i\pm \mid \gamma^\mu \mid j\pm\rangle\langle k\pm \mid \gamma_\mu \mid l\pm\rangle = 2[ik]\langle lj\rangle \qquad \langle k\pm \mid \gamma^\mu \mid l\pm\rangle = \langle l\mp \mid \gamma^\mu \mid k\mp\rangle \tag{2.22}$$

$$\langle ij\rangle\langle kl\rangle = \langle ik\rangle\langle lj\rangle + \langle il\rangle\langle kj\rangle \qquad [ij][kl] = [ik][jl] + [il][kj] \tag{2.23}$$

$$\langle i+|\not{k}|j+\rangle = [ik]\langle kj\rangle \qquad \langle i-|\not{k}|j-\rangle = \langle ik\rangle[kj] \tag{2.24}$$

Using the momentum for the partons outlined above and the on-shell condition for the external partons, $|p_i^\perp| = p_i^+ p_i^-$, we have the following:

$$\langle ij\rangle = p_i^\perp\sqrt{\frac{p_j^+}{p_i^+}} - p_j^\perp\sqrt{\frac{p_i^+}{p_j^-}}, \qquad \langle ai\rangle = -i\sqrt{-\frac{p_a^+}{p_i^+}}p_i^\perp, \qquad \langle ib\rangle = i\sqrt{-p_b^- p_i^+}, \qquad \langle ab\rangle = -\sqrt{\hat{s}}, \tag{2.25}$$

where $\hat{s}$ is the partonic centre of mass energy. In the MRK limit equation 19 simplifies to:

$$\langle ij\rangle \approx -p_j^\perp\sqrt{\frac{p_i^+}{p_j^-}}, \qquad \langle ai\rangle \approx -i\sqrt{\frac{p_a^+}{p_i^+}}p_i^\perp, \qquad \langle ib\rangle \approx i\sqrt{p_i^+ p_n^-}, \qquad \langle ab\rangle \approx -\sqrt{p_1^+ p_n^-}. \tag{2.26}$$

2.5.1 Spinor-Helicity Calculations with Massive Partons

To do calculations with massive partons using the spinor-helicity formalism we must be very careful since all of our favourite identities and tricks rely on the spinor brackets, $|i\rangle$, representing massless partons with $p_i^2 = 0$. We begin by defining 'fundamental spinors' [**?**] which we can use to build more general spinors and go from there.

For some k_0, k_1 satisfying $k_0^2 = 0$, $k_1^2 = -1$ and $k_0 \cdot k_1 = 0$ we can define positive

and negative helicity spinors as follows:

$$u_-(k_0)\overline{u}_-(k_0) \equiv \omega_- \not{k}_0 \tag{2.27a}$$

$$u_+(k_0) \equiv \not{k}_1 u_-(k_0), \tag{2.27b}$$

where $\omega_\lambda = \frac{1}{2}(1 + \lambda\gamma^5)$ is the helicity projection operator. In order for these to be valid spinors they must satisfy the following completeness relations:

$$\sum_\lambda u_\lambda(p)\overline{u}_\lambda(p) = \not{p} + m \tag{2.28a}$$

$$u_\lambda(p)\overline{u}_\lambda(p) = \omega_\lambda \not{p} \tag{2.28b}$$

The spinors in equation can easily be shown to satisfy these as follows:

$$\begin{aligned}
u_-(k_0)\overline{u}_-(k_0) + u_+(k_0)\overline{u}_+(k_0) &= \omega_- \not{k}_0 + \not{k}_1 u_-(k_0)\overline{u}_-(k_0)\not{k}_1, \\
&= \omega_- \not{k}_0 + \not{k}_1 \omega_- \not{k}_0 \not{k}_1, \\
&= \omega_- \not{k}_0 + \frac{1}{2}\gamma^\mu k_{1\mu}(1-\gamma^5)\gamma^\nu k_{0\nu}\gamma^\sigma k_{1\sigma}, \\
&= \omega_- \not{k}_0 + \frac{1}{2}k_{1\mu}k_{0\nu}k_{1\sigma}(\gamma^\mu\gamma^\nu\gamma^\sigma - \gamma^\mu\gamma^5\gamma^\nu\gamma^\sigma), \\
&= \omega_- \not{k}_0 + \frac{1}{2}k_{1\mu}k_{0\nu}k_{1\sigma}(2\gamma^\mu g^{\nu\sigma} - \gamma^\mu\gamma^\sigma\gamma^\nu + 2\gamma^5\gamma^\mu g^{\nu\sigma} - \gamma^5\gamma^\mu\gamma^\sigma\gamma^\nu), \\
&= \omega_- \not{k}_0 + k_{1\mu}k_{0\nu}k_{1\sigma}\omega_+\gamma^\mu(2g^{\nu\sigma} - \gamma^\sigma\gamma^\nu), \\
&= \omega_- \not{k}_0 + 2\not{k}_1 k_0 \cdot k_1 - \omega_+ \not{k}_1 \not{k}_1 \not{k}_0, \\
&= \omega_- \not{k}_0 + \omega_+ \not{k}_0,
\end{aligned}$$

where we have used $\gamma^\mu, \gamma^\mu = 2g^{\mu\nu}$, $\gamma^\mu, \gamma^5 = 0$ and $\not{k}_1\not{k}_1 = k_1^2 = 0$. This proves the property of equation 2.28b and inserting the definition of ω_λ gives:

$$\begin{aligned}
u_-(k_0)\overline{u}_-(k_0) + u_+(k_0)\overline{u}_+(k_0) &= \frac{1}{2}(1-\gamma^5)\not{k}_0 + (1+\gamma^5)\not{k}_0, \\
&= \not{k}_0,
\end{aligned}$$

Which is equation 2.28a for a massless particle.

We can use these fundamental spinors to form spinors for any given momenta, p (which has $p^2 = 0$), as follows:

$$u_\lambda(p) = \not{p} u_{-\lambda}(k_0) \frac{1}{\sqrt{2p \cdot k_0}}, \tag{2.31}$$

provided we dont have $p \cdot k_0 = 0$. Once again it is easy to show that this spinor satisyfies the neccesary conditions, for example:

$$\begin{aligned}
u_\lambda(p)\overline{u}_\lambda(p) &= \frac{1}{2p \cdot k_0} \not{p} u_{-\lambda}(k_0)\overline{u}_{-\lambda}(p)\not{p}, \\
&= \frac{1}{2p \cdot k_0} \not{p}\omega_{-\lambda}\not{k}_0\not{p}, \\
&= \frac{1}{4p \cdot k_0} \not{p}(1 - \lambda\gamma^5)\not{k}_0\not{p}, \\
&= \frac{1}{2p \cdot k_0} p_\mu k_{0\nu} p_\sigma \omega_\lambda \gamma^\mu (2g^{\nu\sigma} - \gamma^\sigma\gamma^\nu), \\
&= \frac{1}{2p \cdot k_0} \omega_\lambda (2\not{p} p \cdot k_0 - \not{p}\not{p}\not{k})), \\
&= \omega_\lambda \not{p}.
\end{aligned}$$

So far so good. This can also be generalised so that we can build massive spinors from our fundamental ones. We can use

$$u(q, s) = \frac{1}{\sqrt{2q \cdot k}} (\not{q} + m) u_-(k) \tag{2.33}$$

to describe a quark with spin 4-vector s, mass m and momentum q. To confirm this we go through the same procedure as above:

$$
\begin{aligned}
u_\lambda(p,s)\overline{u}_\lambda(p,s) &= \frac{1}{2q\cdot k_0}(\not{q}+m)u_-(k_0)\overline{u}_-(q)(\not{q}+m),\\
&= \frac{1}{2q\cdot k_0}(\not{q}+m)\omega_-\not{k}_0(\not{q}+m),\\
&= \frac{1}{4q\cdot k_0}(\not{q}+m)(1-\gamma^5)\not{k}_0(\not{q}+m),\\
&= \frac{1}{4q\cdot k_0}\left[\left(\not{q}\not{k}_0\not{q}+m\not{k}\not{q}+m\not{q}\not{k}_0+m^2\not{k}\right)-\gamma^5\left(\not{q}\not{k}\not{q}-m\not{k}\ slashedq+m\not{q}\not{k}_0-m^2\right.\right.\\
&= \frac{1}{2}\left(\not{q}+m-\gamma^5\not{q}-m\gamma^5+\frac{m\gamma^5\not{k}\not{q}}{k\cdot q}+\frac{\gamma^5 m^2\not{k}}{k\cdot q}\right),\\
&= \frac{1}{2}\left(1+\left(\frac{1}{m}\not{q}-\frac{m}{q\cdot k}\not{k}\right)\gamma^5\right)(\not{q}+m),\\
&= \frac{1}{2}\left(1+\not{s}\gamma^5\right)(\not{q}+m),
\end{aligned}
$$

Where the last line defines the spin vector $s = \frac{1}{m}q - \frac{m}{q\cdot k}k$. Conjecturing a similar form for an antiquark spinor with with spin 4-vector s, mass m and momentum q:

$$
v(q,s) = \frac{1}{\sqrt{2q\cdot k}}(\not{q}-m)u_-(k), \tag{2.35}
$$

which leads to:

$$
\begin{aligned}
v_\lambda(p,s)\overline{v}_\lambda(p,s) &= \frac{1}{2q\cdot k_0}(\not{q}-m)u_-(k_0)\overline{u}_-(q)(\not{q}-m),\\
&= \frac{1}{2}\left(\left(\not{q}-m\right)+\left(-\not{q}+m+\frac{m^2}{q\cdot k_0}\not{k}_0-\frac{m}{q\cdot k_0}\not{q}\not{k}_0\right)\gamma^5\right),\\
&= \frac{1}{2}\left(1+\not{s}\gamma^5\right)(\not{q}-m).
\end{aligned}
$$

One last check that is worth performing is that these spinors actually satisfy the Dirac equation for both the quark and antiquark case. For the quark:

$$\begin{aligned} \not{q}u(q,s) &= \frac{1}{2q\cdot k_0}\not{q}(\not{q}+m)u_-(k_0), \\ &= \frac{1}{2q\cdot k_0}(m^2+m\not{q})u_-(k_0), \end{aligned}$$

we now define some momentum $\widetilde{q}$ by the relation $q=\widetilde{q}+k_0$ such that $\widetilde{q}^2=0$ and $q\cdot k=\widetilde{q}\cdot k$. Since $q^2=2\widetilde{q}\cdot k=m^2$ we may write

$$\begin{aligned} \not{q}u(q,s) &= \frac{1}{m}(m^2+m\not{q})u_-(k_0), \\ &= (m+\not{q})u_-(k_0), \end{aligned}$$

we can now back substitute from the definition of $u(q,s)$ in equation 2.33 to get:

$$\begin{aligned} \not{q}u(q,s) &= \sqrt{2q\cdot k}u(q,s), \\ &= mu(q,s), \end{aligned}$$

which is the Dirac equation for a quark. The result for antiquarks follows similarly.
Now we have forms for massive quarks and antiquarks in terms of massless spinors we can use all of the spinor-helicity machinery to make our computations more efficient. Slightly more useful forms of equations 2.33 and 2.35 can be found by decomposing q in to massless components once again: $q=\widetilde{q}+k$ (once again this acts as a definition for $\widetilde{q}$). Then from equation 2.33:

$$
\begin{aligned}
u(q,s) &= \frac{1}{m}(\not{q} + \not{k} + m)u_-(k), \\
&= \frac{1}{m}\left(|\widetilde{q}^+\rangle\langle\widetilde{q}^+|k^-\rangle + |\widetilde{q}^-\rangle\langle\widetilde{q}^-|k^-\rangle + |k^-\rangle\langle k^-|k^-\rangle + |k^-\rangle\langle k^-|k^-\rangle + m|k^-\rangle\right), \\
&= \frac{[\widetilde{q}k]}{m}|\widetilde{q}^+\rangle + |k^-\rangle,
\end{aligned}
$$

and similarly for the other helicities and the antiquarks:

$$u(q,-s) = \frac{\langle\widetilde{q}k\rangle}{m}|\widetilde{q}^-\rangle + |k^+\rangle, \tag{2.41a}$$

$$v(q,s) = \frac{[\widetilde{q}k]}{m}|\widetilde{q}^+\rangle - |k^-\rangle, \tag{2.41b}$$

$$v(q,-s) = \frac{\langle\widetilde{q}k\rangle}{m}|\widetilde{q}^-\rangle - |k^+\rangle \tag{2.41c}$$

2.6 Monte Carlo Techniques

2.6.1 One Dimensional Integration

Integrals are ubiquitous in every field of physics and particle physics is no different. We have already seen many examples where meaningful physical results can only be obtained after computing an integral two good examples of this are the convolution of the parton distribution functions with the partonic cross-section seen in section **??** and the more complex multi-dimensional integrals seen in section **??** the calculation of the one-loop correction to quark-antiquark production.

For some of the integrals derived here it is not always feasible (and sometimes not even possible) to calculate them analytically. In these situations we must use a numerical approach to approximate the full result. Such approaches generally fall in to one of two categories; quadrature or Monte-Carlo random sampling approaches. The most appropriate solution depends the integrand itself (and in particular our prior knowledge of the integrand) and the number of dimensions we are integrating over.

Here we briefly consider the one-dimensional case. Given an integral:

$$I = \int_a^b f(x)dx, \tag{2.42}$$

we can use well known results such as the Compound Simpson's Rule to approximate the integral by

$$I \approx \frac{h}{3} \sum_{i=0}^{N/2} (f(x_{2i-2}) + 4f(x_{2i-1}) + f(x_{2i})) + \mathcal{O}(N^{-4}), \tag{2.43}$$

where N is the number of times we have subdivided the integral range (a, b) and $x_i = a + \frac{i(b-a)}{N}$ are the points at which we sample the integrand. The error quoted on equation 2.43 only shows the dependence on the sampling rate and it should be noted that there are other factors arising from the size of the domain of integration and on derivatives of the integrand, $f(x)$. The N^{-4} scaling of the error in this method makes it a good choice for numerics in one-dimension.

The Monte-Carlo approach to approximating 2.42 would be to (pseudo-)randomly select a series of N points, x_i, from within the domain of integration and then compute the integral as follows:

$$I \approx I_{MC} = \frac{b-a}{N} \sum_{i=0}^{N} f(x_i) + \mathcal{O}(N^{-\frac{1}{2}}). \tag{2.44}$$

Convergence of this result is assured by the weak law of large numbers (also known as Bernoulli's Theorem) which states that for a series of independent and identically distributed random variables, $X_1, \ldots, X_N$, each with $\mathbb{E}(X_i) = \mu$ the sample mean approaches the population mean as $N \to \infty$. That is,

$$\lim_{N\to\infty} \frac{X_1 + \cdots + X_N}{N} = \mu. \tag{2.45}$$

We can see this explicitly since the expectation of I_{MC} under the continuous probability density function p is:

$$\begin{aligned}\mathbb{E}_p[I_{MC}] &= \mathbb{E}_p\left[\frac{b-a}{N}\sum_{i=0}^{N} f(x_i)\right] \\ &= \frac{b-a}{N}\sum_{i=0}^{N}\mathbb{E}_p\left[f(x_i)\right] \\ &= \frac{b-a}{N}\sum_{i=0}^{N}\int_{-\infty}^{+\infty} f(x)p(x)dx\end{aligned}$$

Where $p(x) = \frac{1}{b-a}$ is the uniform probability distribution for $x \in (a, b)$, hence

$$\begin{aligned}&= \frac{b-a}{N}\frac{1}{b-a}\sum_{i=0}^{N}\int_{a}^{b} f(x)dx \\ &= \int_{a}^{b} f(x)dx = I.\end{aligned}$$

Since the convergence of the Monte-Carlo approximation clearly scales significantly worse that the case for quadrature it would seem that it is not worth considering and, indeed, for low numbers of dimensions it is not. However, this is not the case when considering integrals in dimension $d \geq 2$.

2.6.2 Higher Dimensional Integration

In the case of higher dimensional integrals e.g.

$$I = \int_{[a,b]} f(\vec{x})d\vec{x} = \int_{x_1=a_1}^{x_1=b_1}\cdots\int_{x_n=a_n}^{x_n=b_n} f(x_1,\ldots,x_n)dx_1\ldots dx_n, \tag{2.46}$$

we can still look to generalisations of the quadrature methods touched on in section 2.6.1 however the convergence of these methods is less favourable. Quadrature methods have errors which scale with the number of dimensions we are integrating over, e.g. $\mathcal{O}(N^{-\frac{4}{d}})$ for the compound Simpson's rule. We can argue this intuitively since if we have N points in one dimension to get an error which scales as $\mathcal{O}(N^{-4})$ then in two dimensions we would require N^2 to achieve the same density of samplings and hence $N^2 \sim \mathcal{O}(N^{-4}) \implies N^2 \sim \mathcal{O}(N^{-\frac{4}{2}})$ and more generally $\mathcal{O}(N^{-\frac{4}{d}})$.

By comparison the error of a Monte Carlo approximate stays fixed at $\mathcal{O}(N^{-\frac{1}{2}})$ regardless of the number of dimensions in the problem integrals. We are spared from this so-called 'curse of dimensionality' by the Central Limit Theorem which states that for a sequence of independent and identically distributed random variables $X_1, \ldots, X_N$ each with variance σ^2 we have:

$$\frac{X_1 + \cdots + X_N - N\mathbb{E}(X_1)}{\sqrt{N}\sigma} \xrightarrow{\lim N\to\infty} \mathcal{N}(0,1), \tag{2.47}$$

where $\mathcal{N}(0,1)$ is the normal distribution with mean zero and variance 1. Then using the additive and multiplicative scaling of the normal distribution we see that:

$$\sum_{i=1}^{N} X_i \xrightarrow{\lim N\to\infty} \mathcal{N}\left(\mu, \frac{\sigma^2}{N}\right), \tag{2.48}$$

where μ is the mean of the variables X_i. The variance of a normal distribution is well known and we can use this to see that for a d-dimensional integral we can approximate our uncertainty as:

$$\int_{[a,b]} f(\vec{x})d\vec{x} = V\langle f\rangle \pm V\sqrt{\frac{\langle f\rangle^2 - \langle f^2\rangle}{N}} \tag{2.49}$$

$$\equiv V\langle f\rangle \pm V\frac{\sigma_{MC}}{\sqrt{N}}, \tag{2.50}$$

where V is the volume of the domain of integration, $\langle f\rangle = \sum_i f(x_i)$ and $\langle f^2\rangle = \sum_i f(x_i)^2$.

2.6.3 Variation Reduction Techniques

In equation 2.50 we saw that the error estimate of a Monte Carlo approximation depends no only on the number of points sampled, N, but also on σ_{MC}. We can try to reduce σ_{MC} by reducing how 'variable' the integrand is, for instance in the extreme example where our integrand is $f(x) = f_0$, a constant, it is clear that one Monte Carlo sample is sufficient to compute the integral exactly. Previously when computing $\mathbb{E}_p[I_{MC}]$ we used a uniform probability density function but we are free to use any distribution we like to perform the integration. This can be seen since:

$$\begin{aligned}\mathbb{E}_p[I_{MC}] &= \int f(x)p(x)dx, \\ &= \int \frac{f(x)p(x)q(x)}{q(x)}, \\ &= \mathbb{E}_q\left[\frac{I_{MC}p(x)}{q(x)}\right],\end{aligned}$$

where $q(x)$ is our 'importance sampling' distribution. For example let us consider the integral

$$I = \int_{-5}^{+5} e^{-3|x|}. \tag{2.51}$$

The integrand of equation 2.51 is shown in figure 2.1 along with two potential choices of density functions. Clearly the uniform distribution (shown in red) will sample the integrand equally across the domain however it is clear from looking at the functional form of 2.51 that that isn't the most efficient approach since it is strongly peaked near $x = 0$ and hence that is where the largest contribution to the integral will come from. However if we sample the modified integrand using pseudo-random numbers generated from $\mathcal{N}(0, 0.5)$ (shown in green in figure 2.1) we can reduce the variance of our approximation significantly. Table 2.1 shows how the approximation improves as we vary N for the two cases of $q \sim \mathcal{U}(-5, 5)$ and $q \sim \mathcal{N}(0, 0.5)$.

N	$q \sim \mathcal{U}(-5, 5)$	$q \sim \mathcal{N}(0, 0.5)$
10^1	1.0 ± 0.1	1.0 ± 0.1
10^2	1.0 ± 0.1	1.0 ± 0.1
10^3	1.0 ± 0.1	1.0 ± 0.1
10^4	1.0 ± 0.1	1.0 ± 0.1

Table 2.1: The Monte-Carlo approximation to equation 2.51 as we vary the number of sampled points, N, shown in the naive sampling case and in the importance sampled case.

Table 2.1 clearly shows the value of an importance sampling approach as convergence to the correct result of 1234 is much faster than when we sampled

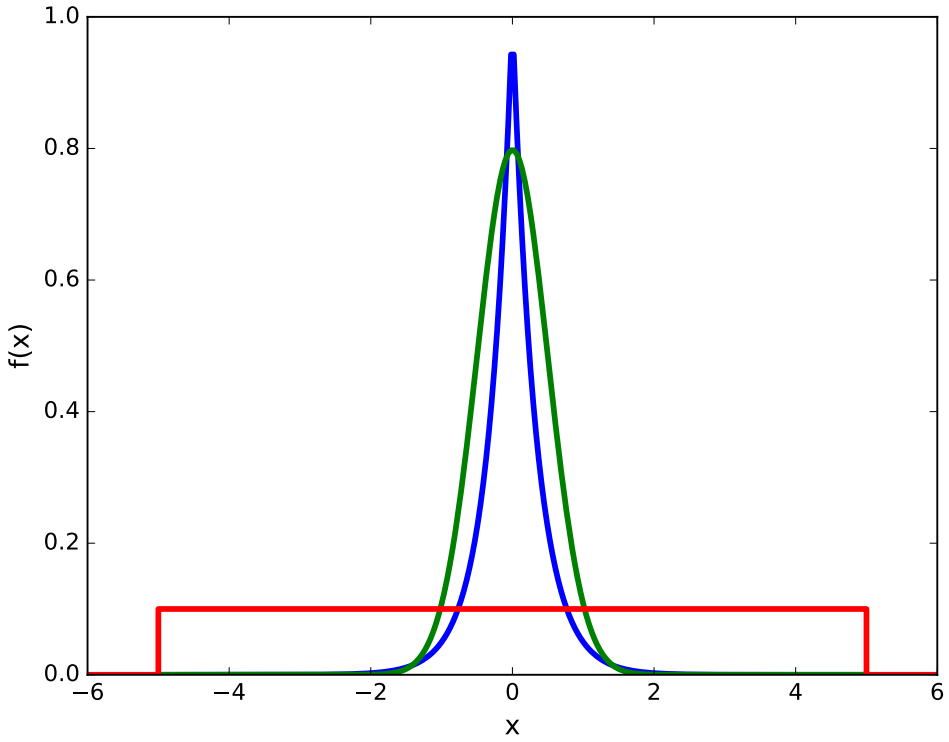

Figure 2.1: A simple importance sampling example (see equation 2.51). The integrand, $f(x)$, is shown in blue, the importance sampling distribution is shown in green and, for comparison, the uniform probability density function used in the naive case of no importance sampling is also shown (in red).

uniformly. This approach relies on us having some prior knowledge of the behaviour of our integrand in order to select the correct probability density function to use[2]. A more realistic, and relevant, example of importance sampling comes from the cross-section for the production of a Z^0 boson in association with dijets. The matrix element squared for such a process will have following form upon factoring out the Z^0 propagator squared:

$$|\mathcal{M}_{Z^0+jj}|^2 \sim \left|\frac{1}{p_Z^2 - M_Z^0 + i\Gamma_Z M_Z}\right|^2 \times f(\text{QCD, EW}) \times g(\text{Kinematic}), \quad (2.52)$$

where p_Z is the momentum carried by the Z^0 boson, M_Z is its mass, Γ_Z is its width and f(QCD, EW) will contain all of the coupling information and g(Kinematic) encodes the remainder of the matrix element. When using a Monte-Carlo approach to generate events of this kind we can use the schematic of 2.52 to *a priori* select an appropriate probability density function to sample from. Figure 2.2 shows the squared Z^0 propagator. Obvious comparisons with figure 2.1 can be drawn in the sense that were we to generate events with a uniform spread of values for p_Z^2 we would end with a very slow rate of convergence by oversampling areas where the integrand is very small and slowly varying.

Another good example of importance sampling is found in how we sample the incoming partons in our simulations. Simple momentum conservation considerations lead us to values for the Bjorken scaling variables of our incoming partons, x_a and x_b, and we can use these to intelligently sample the available partons. The naive way to perform the sum over all possible incoming states would be to uniformly choose a random number corresponding to one of the light quarks, one the light anti-quarks or to a gluon[3]. We can, however, do better than this by using what we know about how the parton density functions vary with $x_{a/b}$ - figure **??** shows this behaviour as measured by ***who?***. By choosing to randomly sample then incoming parton types according to the relative values for the parton density functions we can, once again, reduce the variance of our

[2]More novel approaches whereby the sampling distribution is modified to improve convergence as the Monte-Carlo iterations are calculated, such as the `VEGAS` algorithm exist but they will not be discussed here.

[3]By 'light (anti-)quarks' we mean all except the top and anti-top. The parton density functions for these are not available and, even if they were, they would be small enough that we could safely ignore their contribution to cross-sections.

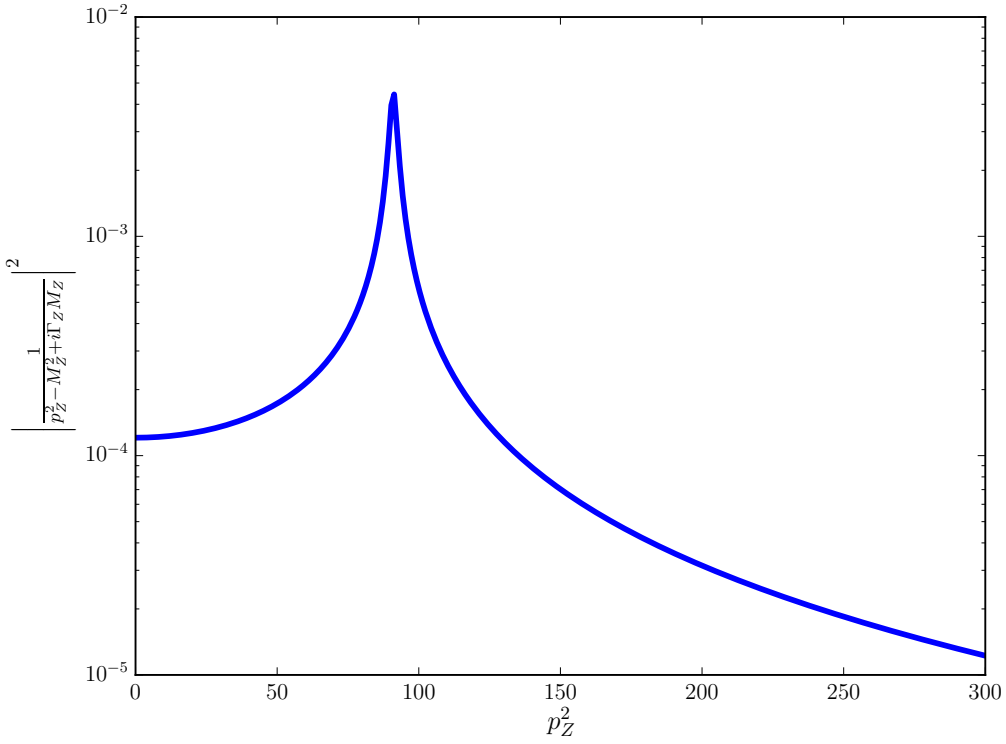

Figure 2.2: The absolute value squared of the Z^0 propagator for a range of values of the invariant mass squared of the Z^0, p_Z^2. We can see it is strongly peaked at the Z^0 mass and, as such, is an ideal candidate for using importance sampling.

numerical integrations as much as possible.

Chapter 3

High Energy QCD

3.1 The High Energy Limit of $2 \to 2$ QCD scattering

3.1.1 Mandelstam Variables in the High Energy Limit

The $2 \to 2$ QCD scattering amplitudes can be expressed in terms of the well-known Mandestam variables s, t and u. Which, in terms of the momenta in the process, are given by:

$$s = (p_1 + p_2)^2 \tag{3.1a}$$

$$t = (p_1 - p_2)^2 \tag{3.1b}$$

$$u = (p_2 - p_3)^3 \tag{3.1c}$$

When working in the high energy limit it is convenient to re-express these in terms of the perpendicular momentum of the outgoing partons, $p_\perp$, and the difference in rapidity between the two final state partons, δy:

$$s = 4p_\perp^2 \cosh^2 \frac{\Delta y}{2} \tag{3.2a}$$

$$t = -2p_\perp^2 \cosh \frac{\Delta y}{2} e^{-\frac{\Delta y}{2}} \tag{3.2b}$$

$$u = -2p_\perp^2 \cosh \frac{\Delta y}{2} e^{\frac{\Delta y}{2}} \tag{3.2c}$$

In the limit of hard jets well separated in rapidity these can be approximated to give

$$s \approx p_\perp^2 e^{\Delta y} \tag{3.3a}$$

$$t \approx -p_\perp^2 \tag{3.3b}$$

$$u \approx -p_\perp^2 e^{\Delta y} \tag{3.3c}$$

From equation (above) it is clear that the 'hard, wide-angle jet' limit is equivalent to the High Energy limit since:

$$\Delta y \approx \ln\left(\frac{s}{-t}\right) \tag{3.4}$$

3.1.2 HE limit of the three-gluon vertex

The three gluon vertex shown in figure (X) has the following Feynman rule:

$$g_s f^{abc}\left((p_1+p_3)^\nu g^{\mu_1\mu_3} + (q-p_3)^{\mu_1} g^{\mu_3\nu} - (q+p_1)^{\mu_3} g^{\mu_1\nu}\right) \tag{3.5}$$

In the high energy limit the emitted gluon with momenta q is much softer that the emitting gluon with momenta p_1 i.e. $p_1^\mu \gg q^\mu \ \forall\mu$ and therefore $p_1 \sim p_3$ - using this we can approximate the vertex by

$$\approx g_s f^{abc}\left(2p_1^\nu g^{\mu_1\mu_3} + p_3^{\mu_1} g^{\mu_3\nu} - p_3^{\mu_3} g^{\mu_1\nu}\right) \tag{3.6}$$

Furthermore, since the hard gluons in a high energy process are external they must satisfy the Ward identities; $\epsilon_1 \cdot p_1 = \epsilon_3 \cdot p_3 = 0$. Hence, the vertex can be expressed simply as:

$$\approx 2g_s f^{abc} p_1^\nu g^{\mu_1\mu_3} \tag{3.7}$$

3.1.3 At Leading Order in α_s

Talk through the limit of $2 \to 2$ scattering of gluons. Introduce mandelstam variables, show the equivalence of large delta y and large s.

3.1.4 At Next-to-Leading Order in α_s

Calculate the NLO calcuations to the 2j ME and show that there explicitly is a delta y (large log) enhancement.

3.1.5 High Energy Jets 'Currents'

3.1.6 Effective Vertices For Real Emissions

3.2 High Energy Jets

3.2.1 The Multi-Regge Kinematic limit of QCD amplitudes

3.2.2 Logarithms in HEJ observables

Here you should take a $2 \to n$ ME, apply the HE limit to it, do a PS integration and show the logs you get. Need the HE limit of PS integral from JA thesis and/or from VDD talk

3.2.3 HEJ currents

Pure Jets

Chapter 4

Z/γ^*+Jets at the LHC

Motivation, other code, experimental papers....

4.1 Z+jets

Similarly to the the case of $W^{\pm}$ plus jets there are *four* possible emission sites for the boson; Two on the forward incoming quark, and two on the backward incoming quarks (see figure 4.1).

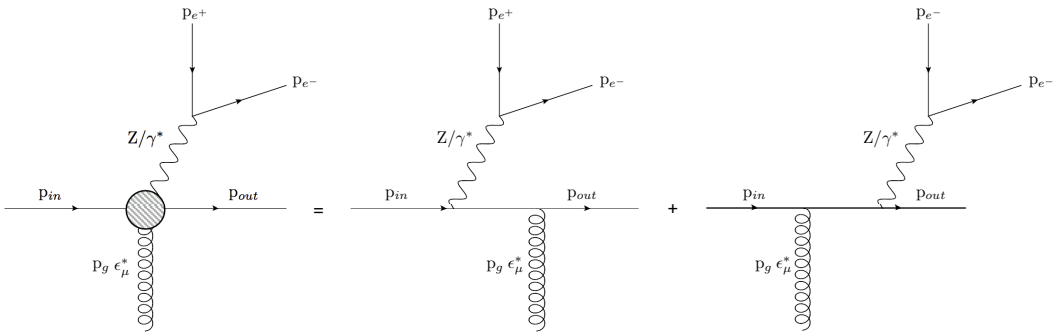

Figure 4.1: The possible emission sites for a neutral weak boson.

In the language of currents (see for *e.g.* [**?**]) we call the left hand side of figure 4.1 j_μ^{Z/γ^*}:

$$j_\mu^Z = \overline{u}^{h_{out}}(p_{out})\left(\gamma^\sigma \frac{\not{p}_{out}+\not{p}_Z}{(p_{out}+p_Z)^2}\gamma_\mu + \gamma_\mu \frac{\not{p}_{in}-\not{p}_Z}{(p_{in}-p_Z)^2}\gamma_\sigma\right) u^{h_{in}}(p_{in}) \times \overline{u}^{h_{e^-}}(p_{e^-})\gamma_\sigma u^{h_{e^+}}(p_{e^+}). \tag{4.1}$$

We can then express amplitudes in terms of contractions of 'emitting' and 'non-emitting' currents.
As the figure above indicates, when emitting a Z boson there is also the possiblity of an off-shell photon being exchanged instead of a Z. Since the difference in these two channels is indistinguishable in the final state we must treat the interference as the amplitude level. For example, the amplitude for $2 \to 2$ scattering is:

$$\mathcal{A}^{2\to 2}_{Z/\gamma^*} = \underbrace{\left(\frac{k_1}{p^2_{Z/\gamma^*} - m^2_Z + i\Gamma_Z m_Z} + \frac{Q_1 e}{p^2_{Z/\gamma^*}}\right)}_{\mathcal{K}_a} \frac{j_1^{Z/\gamma^*} \cdot j_2}{q^2_{t1}} + \underbrace{\left(\frac{k_2}{p^2_{Z/\gamma^*} - m^2_Z + i\Gamma_Z m_Z} + \frac{Q_2 e}{p^2_{Z/\gamma^*}}\right)}_{\mathcal{K}_b} \frac{j_1 \cdot j_2^{Z/} }{q^2_{b1}} \tag{4.2}$$

where k_i are the Z couplings to the quarks, Q_i are the the γ couplings to the quarks, m_Z is the mass of the Z, Γ_Z is the width of the Z peak, q_{t1} is the momentum of the t-channel gluon exchanged when Z emission occurs of the forward incoming quark line and q_{b1} is the momentum of the exchanged gluon when Z emission occurs of the backward incoming quark line.
Equation 4.2 is a good example of the advantages of using currents since the form of the diagrams for either Z or γ can be expressed as only two contraction (with the distinct propagators dealt with in the $\mathcal{K}_i$ terms).
Extra *real* gluon emissions from the t-channel gluon are then included using an effective vertex of the form [**?**][**?**]:

$$V^\rho(q_j, q_{j+1}) = -(q_j + q_{j+1})^\rho - 2\left(\frac{s_{aj}}{s_{ab}} - \frac{q^2_{j+1}}{s_{bj}}\right) p_b^\rho + 2\left(\frac{s_{bj}}{s_{ab}} + \frac{q^2_j}{s_{aj}}\right) p_a^\rho \tag{4.3}$$

Where $s_{aj} = 2p_a \cdot p_j$ *etc.* The general $2 \to n$ amplitude therefore looks like:

$$\mathcal{A}^{2\to n}_{Z/\gamma^*} = \left(\mathcal{K}_a \frac{V^{\mu_1}(q_{t1}, q_{t2}) \cdots V^{\mu_{n-2}}(q_{t(n-1)}, q_{t(n-2)})}{q_{t1} \cdots q_{t(n-1)}} j_1^Z \cdot j_2 + \ldots \right. \tag{4.4}$$
$$\left. \mathcal{K}_b \frac{V^{\mu_1}(q_{b1}, q_{b2}) \cdots V^{\mu_{n-2}}(q_{b(n-1)}, q_{b(n-2)})}{q_{b1} \cdots q_{b(n-1)}} j_1 \cdot j_2^Z \right) \epsilon^*_{\mu_1} \cdots \epsilon^*_{\mu_{(n-2)}}$$

and after taking the modulus squared of this we have the following:

$$|\mathcal{A}^{2\to n}_{Z/\gamma^*}|^2 = \left|\mathcal{K}_a j_1^{Z/\gamma^*}\cdot j_2\right|^2 \frac{V^2(q_{t1},q_{t2})V^2(q_{t2},q_{t3})\cdots V^2(q_{b(n-2)},q_{b(n-1)})}{q^2_{t1}\cdots q^2_{t(n-1)}} + \ldots$$
$$\left|\mathcal{K}_b j_2^{Z/\gamma^*}\cdot j_1\right|^2 \frac{V^2(q_{b1},q_{b2})V^2(q_{b2},q_{b3})\cdots V^2(q_{b(n-2)},q_{b(n-1)})}{q^2_{b1}\cdots q^2_{b(n-1)}} + \ldots$$
$$2\Re\{\mathcal{K}_a\overline{\mathcal{K}_b}\times(j_1^{Z/\gamma^*}\cdot j_2)(\overline{j_2^{Z/\gamma^*}\cdot j_1})\}\frac{V(q_{t1},q_{t2})\cdot V(q_{b1},q_{b2})\cdots V(q_{t(n-2)},q_{t(n-1)})\cdot V(q_{b(n-2)},q_{b(n-1)})}{q_{t1}q_{b1}\cdots q_{t(n-1)}q_{b(n-1)}} \tag{4.5}$$

In previous work it was seen that the interference between forward quark- and backward weak boson emission (the third term in equation 4.5) was negligible [**?**]. This turns out not to be the case in Z plus jets - possibly due to the effects of photon interference.

4.1.1 Formulation in terms of currents

4.1.2 To High Multiplicity Final States

4.1.3 Z^0 Emission Interference

4.1.4 Photonic Interference

4.1.5 The $2 \to n$ Matrix Element

4.1.6 The Differential Z/γ^* Cross-Section

4.2 Regularising the Z/γ^*+Jets Matrix Element

Explain that in the MRK limit the external legs cant (by definition) be soft, then look at the limit of one gluon going soft (basically an NLO correction to the (n-1) parton ME) in the effective vertex. Show that this leads to a divergence.

Next talk about NLO virtual corrections to the (n-1)-parton ME. Show that in the HE limit, only two diagrams contribute (extra t - crosses and uncrossed - g exchange) show the log enhancement given. Give explicity calcultion showing divergences cancelling (as must happen by KLN theorem).

4.2.1 Soft Emissions

To calculate useful quantities such a cross sections *etc.* we must integrate equation 4.5 over all of phase space. However, problems arise when we attempt to integrate over the so called 'soft' (low energy) regions of phase space - things which should be finite diverge and need to be cancelled carefully. It is well understood that the divergences coming from soft *real* emissions cancel with those coming from soft *virtual* emissions and so we must explicitly show this cancellation and calculate the remaining finite contribution multiplying the $(n-1)$-final state parton matrix element.

In the previous work on $W^{\pm}$ emission the finite contribution was found to be [**?**][**?**]:

$$\frac{\alpha_s C_a \Delta_{j-1,j+1}}{\pi} \ln \frac{\lambda^2}{|\vec{q}_{j\perp}|^2}, \tag{4.6}$$

where α_s is the strong coupling strength, C_a is a numerical factor, $\Delta_{i-1,i+1}$ is the rapidity span of the final state partons either side of our soft emission, λ is a factor chosen to define the soft region: $p^2 < \lambda^2$ and $|\vec{q}_{j\perp}|^2$ is the sum of squares of the transverse components of the j^{th} t-channel gluon momenta.

Here we investigate the cancellation of these divergences for Z emission and most importantly whether the finite term is of the same form for the interference term which was previous disregarded.

We start by looking at a $2 \to n$ process and take the limit of one final state parton momentum, p_i, becoming small. Because of the form of equation 4.5 this ammounts to looking at the effect of soft-ness on equation 4.3, we can immediately see that for p_i going soft the gluon chain momenta coming into- and coming out of the j^{th} emission site will coincide: $q_{j+1} \sim q_j$:

$$V^{\rho}(q_j, q_{j+1}) \to -2q_j^{\rho} - 2\left(\frac{s_{aj}}{s_{ab}} - \frac{q_j^2}{s_{bj}}\right) p_b^{\rho} + 2\left(\frac{s_{bj}}{s_{ab}} + \frac{q_j^2}{s_{aj}}\right) p_a^{\rho} \tag{4.7}$$

In equation 4.5 we have two types of terms involving the effective vertex; Terms like $V^2(q_{t/bj}, q_{t/b(j+1)})$ and terms like $V(q_{tj}, q_{t(j+1)}) \cdot V(q_{bj}, q_{b(j+1)})$. The procedure for the V^2 terms doesnt not change between top-line emission and bottom-line emission and so only the calculation for top-line emission will be shown here.

4.2.2 $V^2(q_{tj}, q_{t(j+1)})$ Terms

Once we square equation 4.7 and impose on-shell conditions to p_a and p_b we get:

$$V^2(q_{tj}, q_{tj}) = 4q_j^2 + 8q_j \cdot p_b \left(\frac{s_{aj}}{s_{ab}} - \frac{q_j^2}{s_{bj}}\right) - 8q_j \cdot p_a \left(\frac{s_{bj}}{s_{ab}} + \frac{q_j^2}{s_{aj}}\right) - 4s_{ab}\left(\frac{s_{aj}}{s_{ab}} - \frac{q_j^2}{s_{bj}}\right)\left(\frac{s_{bj}}{s_{ab}} + \frac{q_j^2}{s_{aj}}\right) \tag{4.8}$$

Now since $p_j \to 0$ the terms s_{aj} and s_{bj} will also become vanishing:

$$V^2(q_{tj}, q_{tj}) = 4q_j^2 + 8q_j \cdot p_b \frac{q_j^2}{s_{bj}} - 8q_j \cdot p_a \frac{q_j^2}{s_{aj}} - 4s_{ab}\frac{q_j^4}{s_{bj}s_{aj}} \tag{4.9}$$

Clearly the final term now dominates due to its $\sim \frac{1}{p_i^2}$ behaviour:

$$V^2(q_{ti}, q_{ti}) = -\frac{4s_{ab}}{s_{bi}s_{ai}} q_i^4 + \mathcal{O}\left(\frac{1}{|p_i|}\right) \tag{4.10}$$

We must now explicitly calculate the invariant mass terms. Since we are in the high energy limit we may take $p_a \sim p_1 \sim p_+ = (\frac{1}{2}p_z, 0, 0, \frac{1}{2}p_z)$ and $p_b \sim p_n \sim p_- = (\frac{1}{2}p_z, 0, 0, -\frac{1}{2}p_z)$ and we describe our soft gluon by $p_i = (E, \vec{p})$. Therefore:

$$s_{ai} = 2p_a \cdot p_i \sim 2p_+ \cdot p_i = \frac{1}{2}p_z E - \frac{1}{2}p_z^2, \tag{4.11a}$$

$$s_{bi} = 2p_b \cdot p_i \sim 2p_- \cdot p_i = \frac{1}{2}p_z E + \frac{1}{2}p_z^2, \tag{4.11b}$$

and $s_{ab} = \frac{1}{2}p_z^2$. Then equation 4.10 reads:

$$V^2(q_{ti}, q_{ti}) = -\frac{4p_z^2}{(p_z E - p_z^2)(p_z E + p_z^2)} q_i^4 + \mathcal{O}\left(\frac{1}{|p_i|}\right), \tag{4.12a}$$

$$V^2(q_{ti}, q_{ti}) = -\frac{4p_z^2}{p_z^2(E^2 - p_z^2)} q_i^4 + \mathcal{O}\left(\frac{1}{|p_i|}\right), \tag{4.12b}$$

but since $E^2 - \vec{p}_1^2 = 0$:

$$V^2(q_{ti}, q_{ti}) = -\frac{4}{|\vec{p}_{1\perp}|^2} q_i^4 + \mathcal{O}\left(\frac{1}{|p_i|}\right), \tag{4.13}$$

Now looking back to equation 4.5 we see that each vertex is associated with factors of $(q_{ti}^{-2} q_{t(i+1)}^{-2})$ but once again since the emission is soft this becomes $(q_{ti}^{-4}$. This factor conspires to cancel with that in equation 4.13, moreover each vertex comes with a factor of $-C_A g_s^2$ (which are contained in the $\mathcal{K}_i$ terms in equation

4.5). Including these and dropping subdominant terms the final factor is:

$$\frac{4C_A g_s^2}{|\vec{p}_\perp|^2} \tag{4.14}$$

4.2.3 $V(q_{ti}, q_{t(i+1)}) \cdot V(q_{bi}, q_{b(i+1)})$ Terms

The calculation of the interference term with a soft emission follows similarly to the above section. After taking $p_i \to 0$ and dotting the two vertex terms together we have:

$$\begin{aligned} V(q_{ti}, q_{ti}) \cdot V(q_{bi}, q_{bi}) = 4q_i^t \cdot q_i^b - 4q_i^t \cdot p_a \left(\frac{s_{bi}}{s_{ab}} + \frac{t_i^b}{s_{ai}} \right) + 4q_i^t \cdot p_b \left(\frac{s_{ai}}{s_{ab}} + \frac{t_i^b}{s_{bi}} \right) \dots \\ - 4q_i^b \cdot p_a \left(\frac{s_{bi}}{s_{ab}} + \frac{t_i^t}{s_{ai}} \right) + 4q_i^b \cdot p_b \left(\frac{s_{ai}}{s_{ab}} + \frac{t_i^t}{s_{bi}} \right) \dots \end{aligned} \tag{4.15}$$

having use $p_a^2 = 0$ and $p_b^2 = 0$ once again. We can drop all the terms with s_{ai} or s_{bi} in the denominator and this time we are left with *two* dominant terms which combine to give:

$$V(q_{ti}, q_{ti}) \cdot V(q_{bi}, q_{bi}) = -\frac{s_{ab}}{s_{ai} s_{bi}} t_i^t t_i^b + \mathcal{O}\left(\frac{1}{|p_i|} \right). \tag{4.16}$$

The invariant mass terms here are identical to those we say in the V^2 terms and the products of $t_i^t t_i^b$ also appear in the denominator of the interference term in equation 4.5. After this cancelling we are left with exactly what we had before (see equation 4.14).

Since exactly the same factor comes from all three terms at the amplitude squared level we may factor them out and express the amplitude squared for an n-parton final state with one soft emission in terms of an $(n-1)$-parton final state amplitude squared multiplied by our factor:

$$\lim_{p_i \to 0} |\mathcal{A}_{Z/\gamma^*}^{2 \to n}|^2 = \left(\frac{4C_A g_s^2}{|\vec{p}_{i\perp}|^2} \right) |\mathcal{A}_{Z/\gamma^*}^{2 \to (n-1)}|^2 \tag{4.17}$$

4.2.4 Integration of soft diverences

As mentioned above the divergences only become apparent after we have attempted to integrate over phase space. The Lorentz invariant phase space integral associated with p_i is:

$$\int \frac{d^3\vec{p_i}}{(2\pi)^3 2E_i} \frac{4C_A g_s^2}{|\vec{p}_\perp|^2}. \tag{4.18}$$

It is convenient to replace the integral over the z-component of momentum with one over rapidity, y_2. Rapidty and momentum are realted through:

$$y = \frac{1}{2} \ln \left(\frac{E + p_z}{E - p_z} \right) \tag{4.19}$$

The Jacobian of this transformation is:

$$\frac{dy}{dp_z} = \frac{1}{2(E+p_z)} \frac{\partial}{\partial p_z}(E + p_z) - \frac{1}{2(E-p_z)} \frac{\partial}{\partial p_z}(E - p_z), \tag{4.20}$$

$$= \frac{E}{E^2 - p_z^2} - \frac{p_z}{E^2 - p_z^2} \frac{\partial E}{\partial p_z}, \tag{4.21}$$

$$= \frac{E}{E^2 - p_z^2} - \frac{p_z}{E^2 - p_z^2} \frac{p_z}{E}, \tag{4.22}$$

$$= \frac{1}{E}. \tag{4.23}$$

The phase space integral then reads:

$$\int \frac{d^{2+2\epsilon}\vec{p}_\perp}{(2\pi)^{2+2\epsilon}} \frac{dy}{4\pi} \frac{4C_A g_s^2}{|\vec{p}_\perp|^2} \mu^{-2\epsilon} = \frac{4C_A g_s^2 \mu^{-2\epsilon}}{(2\pi)^{2+2\epsilon} 4\pi} \Delta_{i-1,i+1} \int \frac{d^{2+2\epsilon}\vec{p}_\perp}{|\vec{p}_\perp|^2}, \tag{4.24}$$

where we have analytically continued the integral to $2 + 2\epsilon$ dimensions to regulate the divergence and introduced the parameter μ to keep the coupling dimensionless in the process. Converting to polar cooerdinates and using the result for the volume of a unit hypersphere gives to integrated soft contribution:

$$\frac{4C_A g_s^2}{(2\pi)^{2+2\epsilon} 4\pi} \Delta_{i-1,i+1} \frac{1}{\epsilon} \frac{\pi^{1+\epsilon}}{\Gamma(\epsilon + 1)} \left(\frac{\lambda^2}{\mu^2} \right)^\epsilon \tag{4.25}$$

4.2.5 Virtual Emissions

The virtual emission diagrams are included using the Lipatov ansatz for the gluon propagator:

$$\frac{1}{q_i^2} \longrightarrow \frac{1}{q_i^2} e^{\hat{\alpha}(q_i)(\Delta_{i,i-1})}, \tag{4.26}$$

where:

$$\hat{\alpha}(q_i) = \alpha_s C_A q_i^2 \int \frac{d^{2+2\epsilon}k_\perp}{(2\pi)^{2+2\epsilon}} \frac{1}{k_\perp^2 (k_\perp - q_{i\perp})^2} \mu^{-2\epsilon}. \tag{4.27}$$

Once again we choose to perform the integral using dimensional regularistion. Using the well known Feynman parameterisation formulae gvies:

$$\hat{\alpha}(q_i) = \alpha_s C_A q_i^2 \int \frac{d^{2+2\epsilon}k_\perp}{(2\pi)^{2+2\epsilon}} \int_0^1 \frac{dx}{[x(k-q_i)_\perp^2 + (1-x)k_\perp^2]^2} \mu^{-2\epsilon}, \tag{4.28}$$

$$= \alpha_s C_A q_i^2 \int \frac{d^{2+2\epsilon}\hat{k}_\perp}{(2\pi)^{2+2\epsilon}} \int_0^1 \frac{dx}{[\hat{k}_\perp^2 + q_{i\perp}^2(1-x)]^2} \mu^{-2\epsilon}, \tag{4.29}$$

where we have performed a change of variables to $\hat{k}_\perp = k_\perp - x q_{i\perp}$ with unit Jacobian. Changing the order of integration we can perform the $\hat{k}_\perp$ integral using the following result:

$$\int \frac{d^d k}{(2\pi)^d} \frac{1}{(k^2 - C)^\alpha} = \frac{1}{(4\pi)^{\frac{d}{2}}} \frac{\Gamma(\alpha - \frac{d}{2})}{\Gamma(\alpha)} \frac{(-1)^\alpha}{C^{\alpha - \frac{d}{2}}}, \tag{4.30}$$

to give:

$$\hat{\alpha}(q_i) = \alpha_s C_A q_i^2 \frac{\Gamma(1-\epsilon)}{(4\pi)^{1+\epsilon}} (-q_{i\perp}^2)^{\epsilon-1} \int_0^1 dx (1-x)^{\epsilon-1}, \tag{4.31}$$

$$= -\frac{2 g_s^2 C_A}{(4\pi)^{2+\epsilon}} \frac{\Gamma(1-\epsilon)}{\epsilon} \left(\frac{q_{i\perp}^2}{\mu^2} \right)^\epsilon, \tag{4.32}$$

having completed the x integral and used $\alpha_s = \frac{g_s^2}{4\pi}$.

4.2.6 Cancellation of Infrared Contributions

We now show how the infrared contributions from soft real emissions and virtual emissions cancel leaving our integrated matrix element finite. The subtlety here is that we must sum two diagrams with different final states to see the cancellation. This is because they are experimentally indistinguishable; The $2 \to (n-1)$ virtual diagram has $(n-1)$ resolvable partons in the final state (but is a higher order diagram perturbatively speaking). Because on of the emission in the real $2 \to n$ diagram is soft it is experimentally undetectable so we detect the same final state as the virtual diagram.
The matrix element squared for the real soft diagram will look like:

$$|\mathcal{A}^{2\to n}_{Z/\gamma^*}|^2 = \left(\frac{4g_s^2 C_a}{|p_{i\perp}|^2}\right)\Bigg[\left|\mathcal{K}_a j_1^{Z/\gamma^*}\cdot j_2\right|^2 \frac{\prod_{i\neq j}^{n-2} V^2(q_{ti}, q_{t(i+1)})}{\prod_{i\neq j}^{n-1} q_{ti}^2} + \ldots \tag{4.33}$$

$$\left|\mathcal{K}_b j_2^{Z/\gamma^*}\cdot j_1\right|^2 \frac{\prod_{i\neq j}^{n-2} V^2(q_{bi}, q_{b(i+1)})}{\prod_{i\neq j}^{n-1} q_{bi}^2} + \ldots \tag{4.34}$$

$$2\Re\{\mathcal{K}_a\overline{\mathcal{K}_b}\times(j_1^{Z/\gamma^*}\cdot j_2)(\overline{j_2^{Z/\gamma^*}\cdot j_1})\}\frac{\prod_{i\neq j}^{n-2} V(q_{ti}, q_{t(i+1)})\cdot V(q_{bi}, q_{b(i+1)}))}{\prod_{i\neq j}^{n-1} q_{ti}q_{bi}}\Bigg], \tag{4.35}$$

where we have taken the i^{th} gluon to be soft and the result of the Lorentz invariant phase space integration over the p_i momentum is shown in equation 4.25.
After inserting the Lipatov ansatz into the $2 \to (n-1)$ matrix element squared we have:

$$|\mathcal{A}^{2\to(n-1)}_{Z/\gamma^*}|^2 = \left|\mathcal{K}_a j_1^{Z/\gamma^*}\cdot j_2\right|^2 \frac{\prod_{i}^{n-3} V^2(q_{ti}, q_{t(i+1)})}{\prod_{i}^{n-2} q_{ti}^2} e^{2\hat{\alpha}(q_{ti})\Delta_{i-1,i+1}} + \ldots \tag{4.36}$$

$$\left|\mathcal{K}_b j_2^{Z/\gamma^*}\cdot j_1\right|^2 \frac{\prod_{i}^{n-3} V^2(q_{bi}, q_{b(i+1)})}{\prod_{i}^{n-2} q_{bi}^2} e^{2\hat{\alpha}(q_{bi})\Delta_{i-1,i+1}} + \ldots \tag{4.37}$$

$$2\Re\{\mathcal{K}_a\overline{\mathcal{K}_b}\times(j_1^{Z/\gamma^*}\cdot j_2)(\overline{j_2^{Z/\gamma^*}\cdot j_1})\}\frac{\prod_{i}^{n-3} V(q_{ti}, q_{t(i+1)})\cdot V(q_{bi}, q_{b(i+1)}))}{\prod_{i}^{n-2} q_{ti}q_{bi}} e^{(\hat{\alpha}(q_{bi})+\hat{\alpha}(q_{bi}))} \tag{4.38}$$

We can now go through term-by-term to show the divergences cancel and find the finite contribution to the matrix element squared. Similarly to when we calculated the soft terms the pure top and bottom emissions follow identically so here we will only state the procedure for the top emission. The interference term is slightly different.
For the top line emission we have the following terms:

$$\frac{4C_A g_s^2}{(2\pi)^{2+2\epsilon}4\pi}\Delta_{i-1,i+1}\frac{1}{\epsilon}\frac{\pi^{1+\epsilon}}{\Gamma(\epsilon+1)}\left(\frac{\lambda^2}{\mu^2}\right)^{\epsilon} + e^{2\hat{\alpha_s}(q_{ti})\Delta_{i-1,i+1}}. \tag{4.39}$$

We now extract the relevant term (in terms of the strong coupling order) from the exponential and substitute the expression for $\hat{\alpha}_s$:

$$= \frac{4C_A g_s^2}{(2\pi)^{2+2\epsilon}4\pi}\Delta_{i-1,i+1}\frac{1}{\epsilon}\frac{\pi^{1+\epsilon}}{\Gamma(\epsilon+1)}\left(\frac{\lambda^2}{\mu^2}\right)^{\epsilon} - -\frac{2g_s^2 C_A}{(4\pi)^{2+\epsilon}}\frac{\Gamma(1-\epsilon)}{\epsilon}\left(\frac{q_{ti\perp}^2}{\mu^2}\right)^{\epsilon}, \tag{4.40}$$

$$= \frac{g_s^2 C_A}{4^{1+\epsilon}\pi^{2+\epsilon}}\Delta_{i-1,i+1}\left(\frac{1}{\epsilon\Gamma(1+\epsilon)}\left(\frac{\lambda^2}{\mu^2}\right)^{\epsilon} - \frac{\Gamma(1-\epsilon)}{\epsilon}\left(\frac{q_{ti\perp}^2}{\mu^2}\right)^{\epsilon}\right). \tag{4.41}$$

Expanding the terms involving ϵ yeilds:

$$\frac{1}{\Gamma(1+\epsilon)} = 1 + \gamma_E\epsilon + \mathcal{O}(\epsilon^2), \tag{4.42a}$$

$$\Gamma(1-\epsilon) = 1 + \gamma_E\epsilon + \mathcal{O}(\epsilon^2), \tag{4.42b}$$

$$\left(\frac{x}{y}\right)^{\epsilon} = 1 + \epsilon\ln\left(\frac{x}{y}\right) + \mathcal{O}(\epsilon^2). \tag{4.42c}$$

And so the finite terms are:

$$= \frac{g_s^2 C_A\Delta_{i-1,i+1}}{4^{1+\epsilon}\pi^{2+\epsilon}}\left((1+\gamma_E\epsilon+\mathcal{O}(\epsilon^2))\left(\frac{1}{\epsilon}+\ln\left(\frac{\lambda^2}{\mu^2}\right)+\mathcal{O}(\epsilon)\right) - (1+\gamma_E\epsilon+\mathcal{O}(\epsilon^2))\left(\frac{1}{\epsilon}+\ln\left(\frac{q_{ti\perp}^2}{\mu^2}\right.\right.\right. \tag{4.43a}$$

$$= \frac{g_s^2 C_A\Delta_{i-1,i+1}}{4\pi^2}\ln\left(\frac{\lambda^2}{q_{ti\perp}^2}\right) \tag{4.43b}$$

$$= \frac{\alpha_s C_A\Delta_{i-1,i+1}}{\pi}\ln\left(\frac{\lambda^2}{q_{ti\perp}^2}\right) \tag{4.43c}$$

Likewise for the emission purely from the backward quark line we have:

$$= \frac{\alpha_s C_A \Delta_{i-1,i+1}}{\pi} \ln\left(\frac{\lambda^2}{q_{bi\perp}^2}\right) \tag{4.44}$$

For the interference we expand the exponential with both forward emission q momenta and backward emission q momenta to get:

$$= \frac{g_s^2 C_A \Delta_{i-1,i+1}}{4^{1+\epsilon}\pi^{2+\epsilon}} \left(\left(\frac{1}{\epsilon} + \gamma_E + \ln\left(\frac{\lambda^2}{\mu^2}\right) + \mathcal{O}(\epsilon)\right) - \frac{1}{2}\left[\frac{2}{\epsilon} + 2\gamma_E + \ln\left(\frac{q_{ti\perp}^2}{\mu^2}\right) - \ln\left(\frac{q_{bi\perp}^2}{\mu^2}\right) + \mathcal{O}(\epsilon)\right.\right. \tag{4.45a}$$

$$= \frac{\alpha_s C_A \Delta_{i-1,i+1}}{\pi} \ln\left(\frac{\lambda^2}{\sqrt{q_{ti\perp}^2 q_{bi\perp}^2}}\right) \tag{4.45b}$$

This is a very similar form to that found in [**?**] and [**?**].

4.3 Example: $2 \to 4$ Scattering

As an example we show the cancellation explicitly for the case of $2 \to 4$ when the p_2 momentum has gone soft. A contributing soft diagram is shown in figure 4.2 and one example of a contributing virtual diagram of the same order is shown in figure 4.3. When p_2 goes soft we have the following form for the $2 \to 4$ integrated amplitude squared (N.B.: The integration is only schematic and doesnt represent the full Lorentz invariant phase space):

$$\begin{aligned}\int |\mathcal{A}_{soft}^{2\to 4}|^2 =& \frac{4C_A g_s^2 \Delta_{1,3}}{(2\pi)^{2+2\epsilon} 4\pi} \frac{\pi^{\epsilon+1}}{\epsilon\Gamma(\epsilon+1)} \left(\frac{\lambda^2}{\mu^2}\right)^{\epsilon} \left[|\mathcal{K}_a j_1^Z \cdot j_2|^2 \frac{V^2(q_{t1}, q_{t3})}{q_{t1}^2 q_{t3}^2} + |\mathcal{K}_b j_1 \cdot j_2^Z|^2 \frac{V^2(q_{b1}, q_{b3})}{q_{b1}^2 q_{b3}^2} + \ldots\right. \\ & \left. 2\Re\left\{\mathcal{K}_a \overline{\mathcal{K}_b} (j_1^Z \cdot j_2)\overline{(j_1 \cdot j_2^Z)}\right\} \frac{V(q_{t1}, q_{t3}) \cdot V(q_{b1}, q_{b3})}{q_{t1} q_{t3} q_{b1} q_{b3}}\right],\end{aligned} \tag{4.46}$$

and the virtual contributions for the $2 \to 3$ amplitude is:

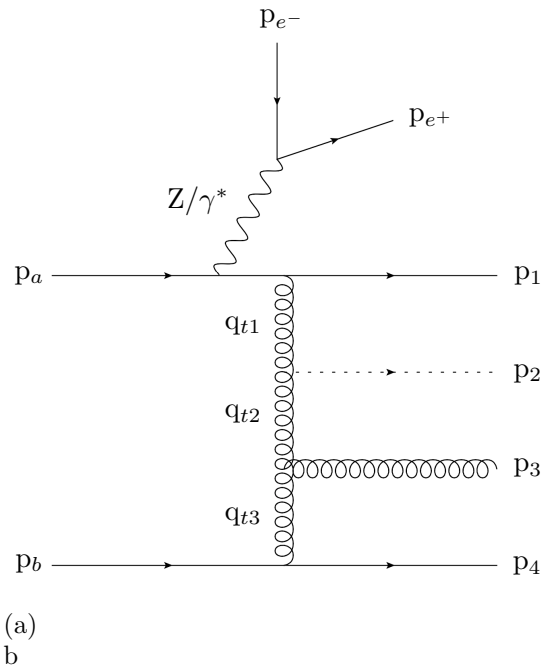

Figure 4.2: Soft Emission

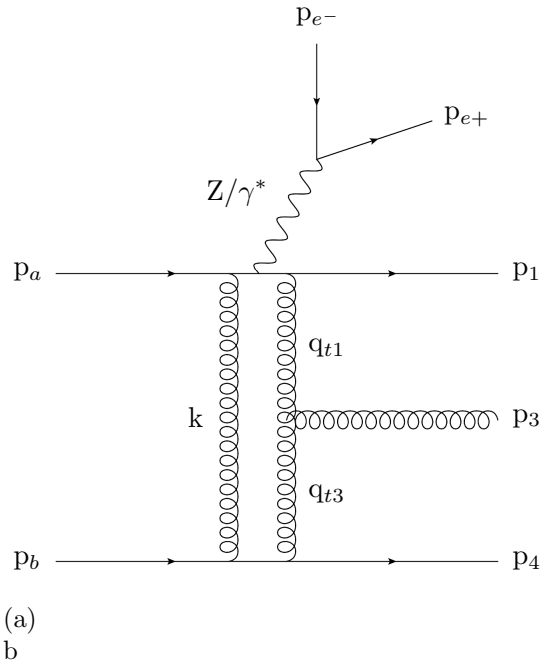

Figure 4.3: Virtual Emission

Figure 4.4: Examples of diagrams contributing to $2 \to 4$ scattering. In figure 4.2 the p_2 has been drawn with a dashed line to denote it is not resolvable. In figure 4.3 the final state momenta have been labelled in a seemingly strange way - this was done to make clear the cancellation when working through the algebra.

$$\int |\mathcal{A}^{2\to 3}_{virtual}|^2 = |\mathcal{K}_b j_1 \cdot j_2^Z|^2 \frac{V^2(q_{t1}, q_{t3})}{q_{t1}^2} e^{2\hat{\alpha}(q_{t1})\Delta_{1,3}} + |\mathcal{K}_t j_1^Z \cdot j_2|^2 \frac{V^2(q_{b1}, q_{b3})}{q_{b1}^2} e^{2\hat{\alpha}(q_{b1})\Delta_{1,3}} + \dots$$
$$2\Re\left\{\mathcal{K}_a \overline{\mathcal{K}_b} (j_1^Z \cdot j_2)\overline{(j_1 \cdot j_2^Z)}\right\} \frac{V(q_{t1}, q_{t3}) \cdot V(q_{b1}, q_{b3})}{q_{t1} q_{t3} q_{b1} q_{b3}} e^{(\hat{\alpha}(q_{t1}) + \hat{\alpha}(q_{b1}))\Delta_{1,3}}. \tag{4.47}$$

Once we expand the exponential to the correct order in g_s^2, the sum of these matrix elements squared over the region of phase space when p_2 is soft is:

$$\int \left(|\mathcal{A}^{2\to 4}_{soft}|^2 + |\mathcal{A}^{2\to 3}_{virtual}|^2\right) = |\mathcal{K}_a j_1^Z \cdot j_2|^2 \frac{V^2(q_{t1}, q_{t3})}{q_{t1}^2} \left(\frac{4C_A g_s^2 \Delta_{1,3}}{(2\pi)^{2+2\epsilon} 4\pi} \frac{\pi^{\epsilon+1}}{\epsilon\Gamma(\epsilon+1)} - 2\hat{\alpha}(q_{t1})\Delta_{1,3}\right) + \dots$$
$$|\mathcal{K}_b j_1 \cdot j_2^Z|^2 \frac{V^2(q_{b1}, q_{b3})}{q_{b1}^2} \left(\frac{4C_A g_s^2 \Delta_{1,3}}{(2\pi)^{2+2\epsilon} 4\pi} \frac{\pi^{\epsilon+1}}{\epsilon\Gamma(\epsilon+1)} - 2\hat{\alpha}(q_{b1})\Delta_{1,3}\right) + \dots$$
$$2\Re\left\{\mathcal{K}_a \overline{\mathcal{K}_b} (j_1^Z \cdot j_2)\overline{(j_1 \cdot j_2^Z)}\right\} \frac{V(q_{t1}, q_{t3}) \cdot V(q_{b1}, q_{b3})}{q_{t1} q_{t3} q_{b1} q_{b3}} \left(\frac{4C_A g_s^2 \Delta_{1,3}}{(2\pi)^{2+2\epsilon} 4\pi} \frac{\pi^{\epsilon+1}}{\epsilon\Gamma(\epsilon+1)} - (\hat{\alpha}(q_{t1}) + \hat{\alpha}(q_{b1}))\Delta_{1,3}\right) \tag{4.48}$$

These bracketed terms are exactly the cancellations calculated in section 4 above. Therefore:

$$\int \left(|\mathcal{A}^{2\to 4}_{soft}|^2 + |\mathcal{A}^{2\to 3}_{virtual}|^2\right) = \frac{\alpha_s C_A \Delta_{1,3}}{\pi} \left(|\mathcal{K}_a j_1^Z \cdot j_2|^2 \frac{V^2(q_{t1}, q_{t3})}{q_{t1}^2} \ln\left(\frac{\lambda^2}{|q_{1t\perp}|^2}\right) + \dots \right.$$
$$|\mathcal{K}_b j_1 \cdot j_2^Z|^2 \frac{V^2(q_{b1}, q_{b3})}{q_{b1}^2} \ln\left(\frac{\lambda^2}{|q_{1b\perp}|^2}\right) + \dots$$
$$\left. 2\Re\left\{\mathcal{K}_a \overline{\mathcal{K}_b} (j_1^Z \cdot j_2)\overline{(j_1 \cdot j_2^Z)}\right\} \frac{V(q_{t1}, q_{t3}) \cdot V(q_{b1}, q_{b3})}{q_{t1} q_{t3} q_{b1} q_{b3}} \ln\left(\frac{\lambda^2}{\sqrt{|q_{1t\perp}|^2 |q_{1b\perp}|^2}}\right) \right) + \mathcal{O}(\alpha_s^2), \tag{4.49}$$

Which is manifestly finite.

Chapter 5

$t\bar{t}$+Jets in the High Energy Limit

Talk about the trivial massless case and the colour factors involved compare to MadGraph. Move to the massive case, talk about the nice momentum decomposition and write down the massive matrix elements.

Chapter 6

High Multiplicity Jets at ATLAS

Show the ATLAS pure jets analysis and talk a bit about the issues with running the damn thing. Talk about the conclusions about BFKL-like dynamics

Chapter 7

The $W^{\pm}$ to Z/γ^{*} Ratio at ATLAS

Compare HEJ Z+Jets to NJet (NLO predictions) and MadGraph (LO predictions)

Chapter 8

Z/γ^*+Jets at 100TeV

Talk about the FCC movement and the effect we expect the resummation will have at these energies

Chapter 9

Conclusions and Outlook

Publications

Author Name(s). Title of publication. In *Where Published*, Year.

Author Name(s). Title of publication. In *Where Published*, Year.